J. Fluid Mech. (1971), *vol.* 47, *part* 2, *pp.* 337–351
Printed in Great Britain

The non-linear evolution of Stokes waves in deep water

By VINCENT H. CHU† AND CHIANG C. MEI
Parsons Laboratory for Water Resources and Hydrodynamics
Massachusetts Institute of Technology

(Received 9 June 1970 and in revised form 22 October 1970)

Based on a set of modulation equations derived in a previous paper, the non-linear evolution of wave envelope in deep water is studied numerically. It is found that the wave envelope tends to disintegrate to multiple groups of waves each of which approaches a stable permanent envelope representing dynamical equilibrium between the amplitude dispersion and the frequency dispersion. Qualitative agreement with the experimental measurements of Feir (1967) is also observed.

1. Introduction

In previous papers (Chu & Mei 1970*a*, *b*) a WKB method was used to derive the modulation equations of Whitham's (1967) type for slowly varying Stokes waves. It was found that terms of dispersive type, neglected in Whitham's theory to the same order of approximation, must be included to extend the validity of these equations. In the limiting case of two-dimensional infinitely deep water, these equations, governing the slow modulation of the wave amplitude a and the wave-number k, may be summarized as follows:

$$\left.\begin{aligned} \frac{\partial}{\partial t}\left(\frac{a^2}{\omega_0}\right) + \frac{\partial}{\partial x}\left(C_g \frac{a^2}{\omega_0}\right) = 0, \\ \frac{\partial k}{\partial t} + \frac{\partial \omega}{\partial x} = 0, \end{aligned}\right\} \tag{1.1a,b}$$

where $\omega_0 = (gk)^{\frac{1}{2}}$ is the first-order approximation for the wave frequency ω and $C_g = g/2\omega_0$ is the group velocity. In (1.1*a*, *b*), (x, t) are the stretched variables which are related to the natural time and space variables (X, T) by

$$(x, t) = \epsilon(X, T), \tag{1.2}$$

where ϵ is a small parameter characterizing both the wave steepness and the slow rate of modulation. The distinction between Whitham's theory and ours lies in the expression for ω; whilst the former implies the direct use of Stokes' dispersion relation for a uniform wave train,

$$\omega = \omega_0(1 + \tfrac{1}{2}\epsilon^2 k^2 a^2), \tag{1.3}$$

† Present address: Department of Civil Engineering and Applied Mechanics, McGill University, Montreal, Canada

we have instead the following

$$\omega = \omega_0[1 + \epsilon^2(\tfrac{1}{2}k^2a^2 + [(a/\omega_0)_{tt}/2\omega_0 a])]. \tag{1.4}$$

It seems desirable to give an elementary argument for the necessity of the additional dispersion term. To this end the classical linear example of beats is again the most effective. We consider the superposition of two sinusoidal waves of equal amplitude a_0 but slightly different wave-numbers k_i and frequencies ω_i $(i = 1, 2)$. The composite wave can be represented as a single wave train with varying wave amplitude $a(x, t)$ and phase $\psi(x, t)$, i.e.

$$\eta(x, t) = a\cos\psi, \tag{1.5}$$

$$\left.\begin{aligned} \text{where} \quad & a(x, t) = 2a_0\cos(\tfrac{1}{2}(k_1 - k_2) \times -\tfrac{1}{2}(\omega_1 - \omega_2)t), \\ \text{and} \quad & \psi(x, t) = \tfrac{1}{2}(k_1 + k_2) = -\tfrac{1}{2}(\omega_1 + \omega_2)t. \end{aligned}\right\} \tag{1.6a, b}$$

The variation of the wave amplitude $a(x, t)$ is slow since

$$\Delta k/k_i, \Delta\omega/\omega_i \ll 1\,(\Delta k = k_1 - k_2, \Delta\omega = \omega_1 - \omega_2).$$

The wave-number and the wave frequency may be defined by the phase ψ as,

$$\left.\begin{aligned} k(x, t) &= \partial\psi/\partial x = \tfrac{1}{2}(k_1 + k_2), \\ \omega(x, t) &= -\partial\psi/\partial t = \tfrac{1}{2}(\omega_1 + \omega_2). \end{aligned}\right\} \tag{1.7a, b}$$

We observe that if the individual sinusoid satisfies a certain dispersion relation $\omega_i = f(k_i)$, it is in general not true that $\omega = f(k)$ except for non-dispersive waves where f is linear in k. In fact, for $\Delta k/k_i$, $\Delta\omega/\omega_i \ll 1$, the following is true

$$\omega = f(k) + \frac{(\Delta k)^2}{8}\frac{d^2f}{dk^2} + O\{(\Delta k)^3\}. \tag{1.8}$$

Since $(\Delta k)^{-1}$ represents the length scale of the envelope modulation, we arrive at the important conclusion that direct use of the plane wave dispersion relation leads to an error that is second order in the modulation rate, in accordance with the twice differentiation of the new term in (1.4).

Based on Whitham's approximation, the non-linear evolution of Stokes waves has been studied by Lighthill (1965, 1967) for a wave packet, and by Howe (1967, 1968) for a steady flow past a slowly modulated wavy wall. Because of the omission just discussed, the amplitude dispersion dominates the entire evolution process and hence their theories show the persistent steepening of the envelope and the occurrence of frequency shocks. As in long waves in shallow water, when distortion due to amplitude dispersion is sufficiently severe, frequency dispersion also becomes more effective in exerting a counteracting influence. Even if shocks should occur, their first occurrence should be widely different from what can be predicted from Whitham's theory. In this sense Whitham's theory is comparable to Airy's while ours is to Boussinesq's for shallow water waves.

The primary purpose of this paper is to investigate the non-linear evolution with both kinds of dispersion for much longer range of time. Numerical methods are used for two types of initial states: (1) a pulse-shaped envelope corresponding to the problem treated theoretically by Lighthill (1965, 1967) and (2) periodic

modulation of a uniform wave train, aiming at the development subsequent to the initial growth of instability (Benjamin & Feir 1967). In the first case comparison with a sample record from Feir's (1967) experiments is also made by accounting for the effect of damping semi-empirically.

2. Reduction of governing equations

In (1.1) the allowed total variations of a and k (or ω) are of order $O(1)$. It is sufficient for present purposes to restrict further the variation of k down to $O(\epsilon)$, i.e.

$$k = \bar{k} + \epsilon\mu, \quad \bar{k} = \text{constant}. \tag{2.1}$$

It then follows from definitions that

$$\left.\begin{aligned} C_g &= \bar{C}_g + \epsilon\mu(d\bar{C}_g/d\bar{k}) + O(\epsilon^2), \quad \bar{C}_g = \tfrac{1}{2}(g/\bar{k})^{\frac{1}{2}}; \\ \omega_0 &= \bar{\omega} + \epsilon\bar{C}_g\mu + \tfrac{1}{2}\epsilon^2\mu^2(d\bar{C}_g/d\bar{k}) + O(\epsilon^3), \quad \bar{\omega} = (g\bar{k})^{\frac{1}{2}}. \end{aligned}\right\} \tag{2.2a,b}$$

Substituting into (1.1a,b) we then have

$$\left.\begin{aligned} &\left(\frac{\partial}{\partial t} + \bar{C}_g\frac{\partial}{\partial x}\right)a^2 + \epsilon\frac{d\bar{C}_g}{d\bar{k}}\frac{\partial}{\partial x}(\mu a^2) = O(\epsilon^2), \\ &\left(\frac{\partial}{\partial t} + \bar{C}_g\frac{\partial}{\partial x}\right)\mu + \epsilon\frac{\partial}{\partial x}\left[\frac{d\bar{C}_g}{d\bar{k}}\tfrac{1}{2}\mu^2 + \tfrac{1}{2}\bar{\omega}\bar{k}^2a^2 - \tfrac{1}{2}\frac{\bar{C}_g^2}{\bar{\omega}}\frac{a_{xx}}{a}\right] = O(\epsilon^2). \end{aligned}\right\} \tag{2.3a,b}$$

This suggests a moving frame of reference following the group velocity $\bar{C}_g$; the following transformation simplifies and non-dimensionalizes the above equations:

$$\left.\begin{aligned} A &= a/\bar{a}, \quad W = \mu/2\bar{k}^2\bar{a} \cong (\omega_0 - \bar{\omega})/\epsilon\bar{\omega}\bar{k}\bar{a}, \\ x' &= \bar{k}^2\bar{a}(x - \bar{C}_g t), \quad t' = \epsilon(\bar{k}\bar{a})^2\bar{\omega}t, \end{aligned}\right\} \tag{2.4}$$

where $\bar{a}$ is a characteristic amplitude to be specified. Equations (2.3a,b) then become:

$$\left.\begin{aligned} &\frac{\partial A^2}{\partial t'} + \frac{\partial}{\partial x'}(-\tfrac{1}{2}WA^2) = 0, \\ &\frac{\partial W}{\partial t'} + \frac{\partial}{\partial x'}\left(-\tfrac{1}{4}W^2 + \tfrac{1}{4}A^2 + \frac{A_{x'x'}}{16A}\right) = 0. \end{aligned}\right\} \tag{2.5a,b}$$

These equations play the same role as the Korteweg–de Vries equation in the shallow water wave theory.

If they are further linearized by letting $A = 1 + \epsilon\alpha$ and $W = \epsilon\beta$, we obtain,

$$\alpha_{t'} - \tfrac{1}{4}\beta_{x'x'} = 0, \beta_{t'} + \tfrac{1}{2}\alpha_{x'} + \tfrac{1}{16}\alpha_{x'x'x'} = 0. \tag{2.6a,b}$$

Equations (2.5a,b) will be used as the basis of our study. Before doing that, some detailed properties of the permanent wave solutions are needed.

3. Permanent waves

These solutions of course represent the special states of dynamic equilibrium between amplitude and frequency dispersion; their existence has been pointed

out before by Benney & Newell (1967). Taking $\partial/\partial t' = 0$ and integrating once, we have

$$\left.\begin{aligned} WA^2 &= C_1 = \text{constant}, \\ -4W^2+4A^2+A_{x'x'}/A &= C_2 = \text{constant}. \end{aligned}\right\} \tag{3.1a,b}$$

Combining and integrating again one easily obtains for $E = A^2$,

$$\begin{aligned} (E_{x'})^2 = f(E) &= -8E^3+4C_2E^2+8C_3E-16C_1^2 \\ &= 8(E_{\max}-E)\,(E-E_{\min})\,(E-E_0), \end{aligned} \tag{3.2}$$

with

$$C_1^2 = -\tfrac{1}{2}E_0E_{\max}E_{\min}, \tag{3.3}$$

whence $E_0 < 0$. Analytically, the solution is

$$E = E_{\min}+(E_{\max}-E_{\min})\,\mathrm{cn}^2\{[2(E_{\max}-E_{\min})]^{\frac{1}{2}}\gamma x'\}, \tag{3.4}$$

with the modulus

$$\gamma^2 = (E_{\max}-E_{\min})/(E_{\max}-E_0). \tag{3.5}$$

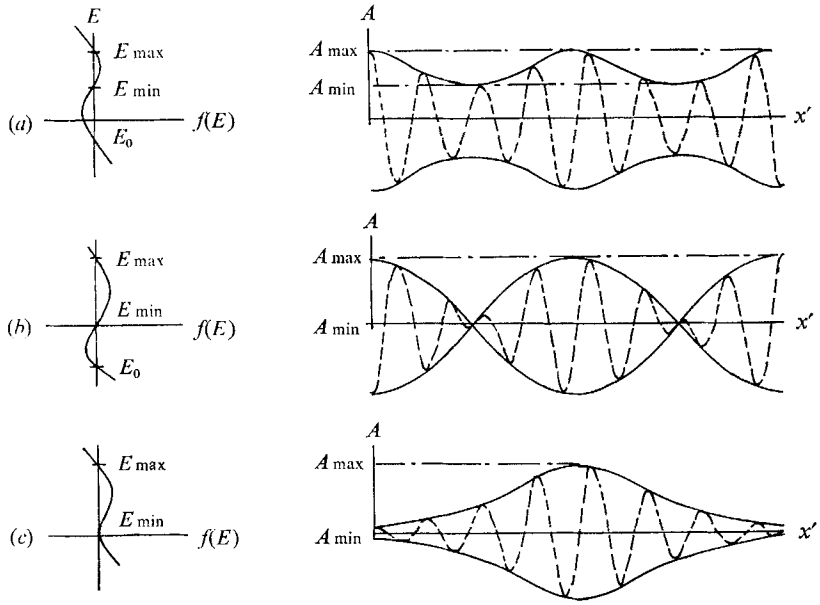

FIGURE 1. Permanent wave envelopes. (*a*) $E_{\min} \neq E_0 \neq 0$. (*b*) $E_{\min} = 0$, $E_0 \neq 0$. (*c*) $E_{\min} = E_0 = 0$.

The wavelength of the envelope is

$$\lambda = \frac{2^{\frac{1}{2}}\gamma}{(E_{\max}-E_{\min})^{\frac{1}{2}}}\int_0^{\frac{1}{2}\pi}\frac{d\xi}{(1-\gamma^2\sin^2\xi)^{\frac{1}{2}}} \tag{3.6}$$

Whilst $E_{\max}$ and $E_{\min}$ specify the amplitude, E_0 specifies the wavelength. The wave-number change W follows from (3.1*a*):

$$W = C_1/E = (1/E)\,[-\tfrac{1}{2}E_0E_{\max}E_{\min}]^{\frac{1}{2}}. \tag{3.7}$$

Now by letting $E = E_{\max}$ in (3.7), $W_{\min}$ is obtained which yields an expression for $\omega_{0\min}/\bar{\omega}$ from the definition. The propagation speed of the envelope is then given by

$$\bar{C}_g = (g/2\omega_{0\min})\,[1+\epsilon k_{\min}a_{\min}(-\tfrac{1}{2}E_0/E_{\max})^{\frac{1}{2}}+O(\epsilon^2)]. \tag{3.8}$$

Possible variations of the envelope form are depicted in figure 1. Some important features in cases (*b*) and (*c*) need stressing. For cases (*b*) and (*c*) $E_{\min} = 0$, $W = 0$, hence the wave-number is uniform throughout and $\omega_0 = \bar{\omega} =$ constant. It implies in turn that $\bar{C}_g =$ constant so that the propagation speed is independent of the amplitude of the envelope. At the nodal points $A^2_{\min} = E_{\min} = 0$ but $(A_{x'})^2 = -2E_{\max}E_0$ as may be inferred from (3.2). Hence $A_{x'} \neq 0$ unless $E_0 = 0$ and the envelope cuts the horizontal axis sharply. If in addition, $E_0 = 0$, then $\gamma \sim 1$ and $\lambda \sim \infty$; (*b*) reduces to (*c*), leading to the solitary envelope on a null background, i.e.

$$A/A_{\max} = \operatorname{sech} 2^{\frac{1}{2}} A_{\max} x' \quad \text{and} \quad W \equiv 0. \tag{3.9}$$

4. Numerical scheme

We employ the following explicit finite-difference scheme for (2.5*a*, *b*):

$$\left.\begin{aligned} A^2_{i,j+1} &= A^2_{i,j-1} + \tfrac{1}{2}(\Delta t'/\Delta x')\,(W_{i+1,j}A^2_{i+1,j} - W_{i-1,j}A^2_{i-1,j}), \\ W_{i,j+1} &= W_{i,j-1} + \tfrac{1}{4}(\Delta t'/\Delta x')\,[(W^2_{i+1,j} - W^2_{i-1,j}) - (A^2_{i+1,j} - A^2_{i-1,j})] \\ &\quad + \frac{1}{16}\frac{\Delta t'}{(\Delta x')^3}\left[\frac{A_{i+2,j} - A_{i,j}}{A_{i+1,j}} - \frac{A_{i,j} - A_{i-2,j}}{A_{i-1,j}}\right]. \end{aligned}\right\} \tag{4.1a,b}$$

Periodic boundary conditions are prescribed at the period $N\Delta x'$, i.e.

$$A_{i+N,j} = A_{i,j}, \quad W_{i+N,j} = W_{i,j}. \tag{4.2a,b}$$

Initial values of A and W are prescribed at $j = 0$. Guidance for the criterion of numerical stability is suggested by the observation that the linearized version (2.6*a*, *b*) is equivalent to the equation governing the vibration of an elastic column under axial compression (Morse 1948, p. 116):

$$\alpha_{t't'} + \tfrac{1}{8}\alpha_{x'x'} + \tfrac{1}{64}\alpha_{x'x'x'x'} = 0, \tag{4.3}$$

for which the stability parameter is known to be $\Delta t'/(\Delta x')^2$ (Richtmyer 1964, p. 185). By numerical trial and error it is found that $\Delta t'/(\Delta x')^2 \leqq 1$ ensures stability in present computations. As a further check a solitary envelope of permanent form is first chosen as the initial value. With $\Delta t' = 0{\cdot}01$, $\Delta x' = 0{\cdot}1$ and $N = 200$, (N is sufficiently large that values at the two spatial ends are negligible) the envelope is found to travel for $500\,\Delta t'$ without appreciable change of form. The change of peak amplitude is 0·3 % and total energy 0·02 %. For all computed cases in §§ 5, 6 energy is conserved within 0·5 %.

5. Evolution of a wave packet

The main intention of this section is to compare with Lighthill's (1967) analysis of a similar problem. Pertinent experiments have also been performed by Feir (1967) which support Lighthill's prediction qualitatively only for a limited initial range of time. We adopt the following initial condition

$$t = 0: \begin{Bmatrix} A(x', 0) = \operatorname{sech} x'/2^{\frac{1}{2}}, \\ W(x', 0) = 0. \end{Bmatrix} \tag{5.1}$$

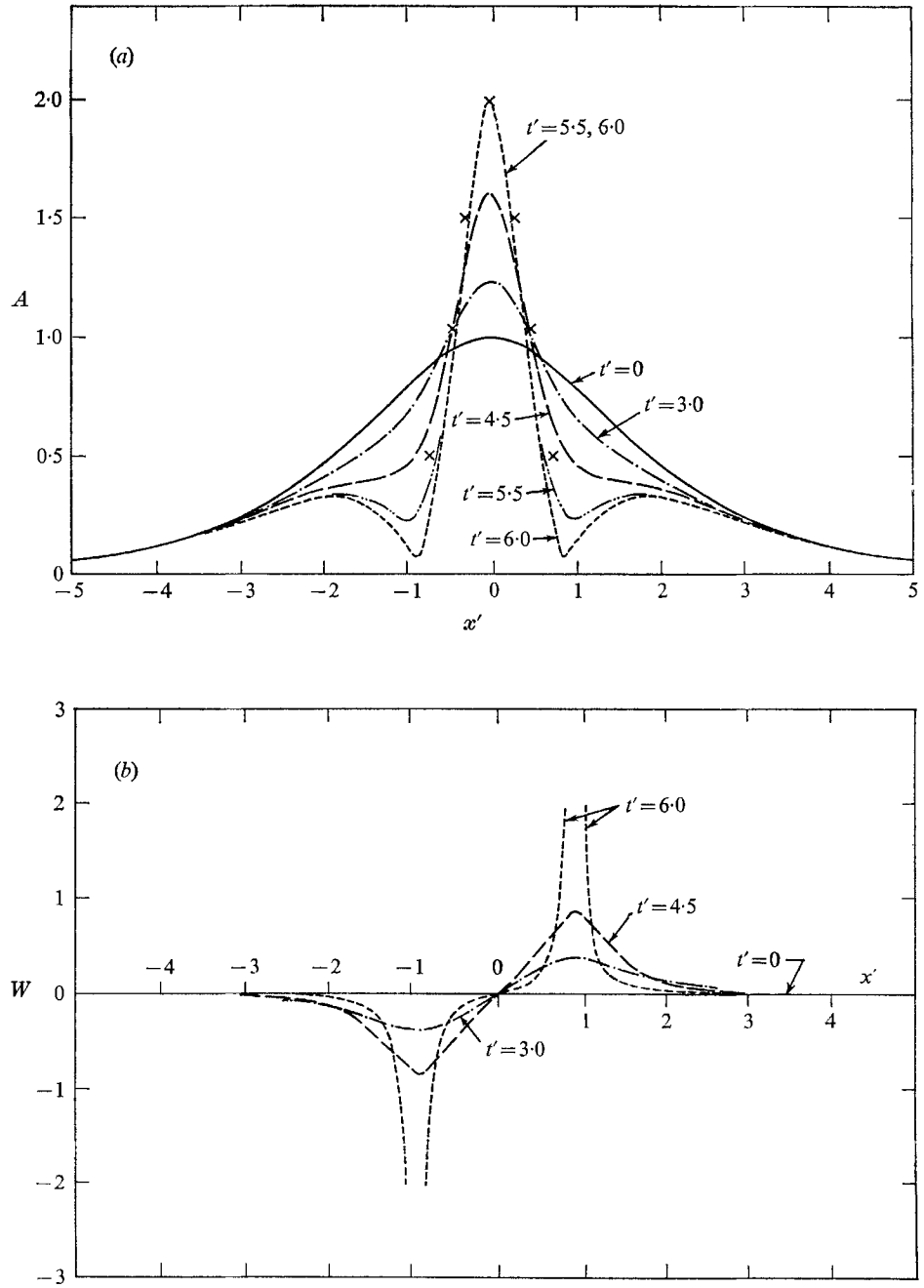

FIGURE 2. Evolution of a symmetrical envelope-pulse with amplitude flatter than a permanent pulse (initially A = sech $x'/2^{\frac{1}{2}}$, $W = 0$ at $t = 0$). $\Delta x' = 0{\cdot}075$, $\Delta t' = 0{\cdot}005$, $N = 300$. (*a*) Amplitude A, ($\times\times\times$): permanent pulse. (*b*) Wave-number spread W. (*c*) Growth rate at the centre of the group.

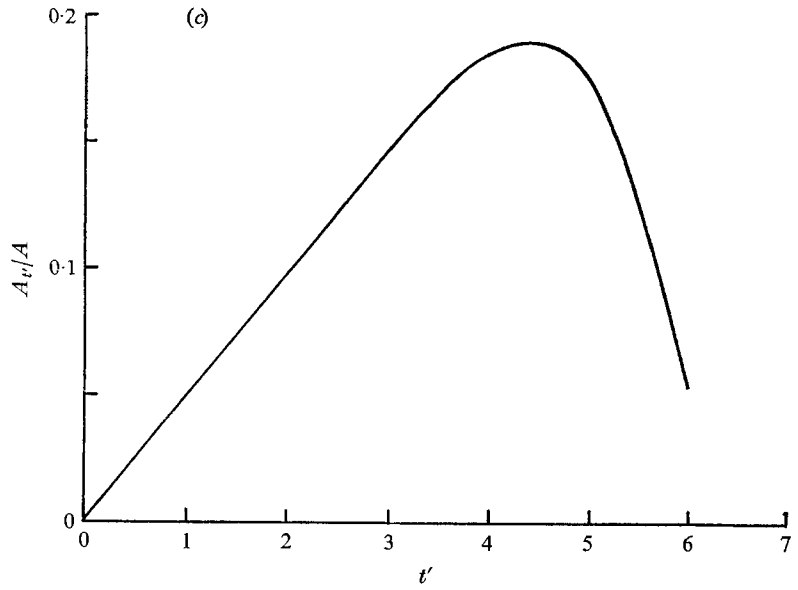

FIGURE 2(c). For legend see facing page.

The results are shown in figure 2. The essential features are that the maximum amplitude first increases and at the same time the wave-number increases in front of but decreases behind the peak. After certain time, separation into groups becomes evident. The primary group approaches a permanent form with a higher peak (in this case it is practically a solitary wave since $\gamma > 0{\cdot}95$), while the wave-number within it returns to uniform. The groups are eventually separated by nodes where sharp peaks of W appear after which the computation cannot proceed. Since the rate of growth of the primary peak *diminishes* as the permanent form is approached, as shown in figure 2(c), it appears that a 'steady state' of dynamical equilibrium can be established.† The sharp wave-number peaks simply suggest that there is a jump of phase there.

The sequence of events can be qualitatively discussed on the basis of (2.5*a*, *b*). First, we display the amplitude-dispersion term $-\frac{1}{4}(A^2)_{x'}$, and the frequency-dispersion term $(\frac{1}{4}W^2-(A_{x'x'}/16A)_{x'}$ in figure 3. If the initial profile is flatter than the equilibrium (permanent) one, amplitude dispersion dominates at the beginning. It follows from (2.5*b*) that $W_{t'}$ is of the shape as in figure 3(*b*), leading to a similar distribution of W. In view of (2.5*a*), $-\frac{1}{2}W$ is the velocity of energy flux, hence energy is convected towards the centre, in agreement with Lighthill (1967). The non-uniformity of flux rate as well as the opposing influence of frequency dispersion are then responsible for the generation of the dimples and the eventual separation on two sides of the peak. Thus, while the nodes are gradually formed, no energy is communicated across them, leading to a final approach to equilibrium.

While the sharpening of the wave-number curve (or fast change of phase) and the formation of nodes may not be accurately predicted here in a quantitative

† In fact, near the time of node formation, appreciable changes occur only around the nodes.

sense due to the slow-modulation assumption, the simultaneous occurrence of the two has been observed in experiments (Feir 1967, figures 1, 2) and is consistent with the tendency towards dynamical equilibrium within the main part of a group. As this tendency must be accompanied by a redistribution of waves such that the wavelength becomes uniform, two given wave crests somewhat away from, and on the opposite sides of, a node cannot in general be perfectly in phase unless under very lucky circumstances. Hence a phase jump must result. The

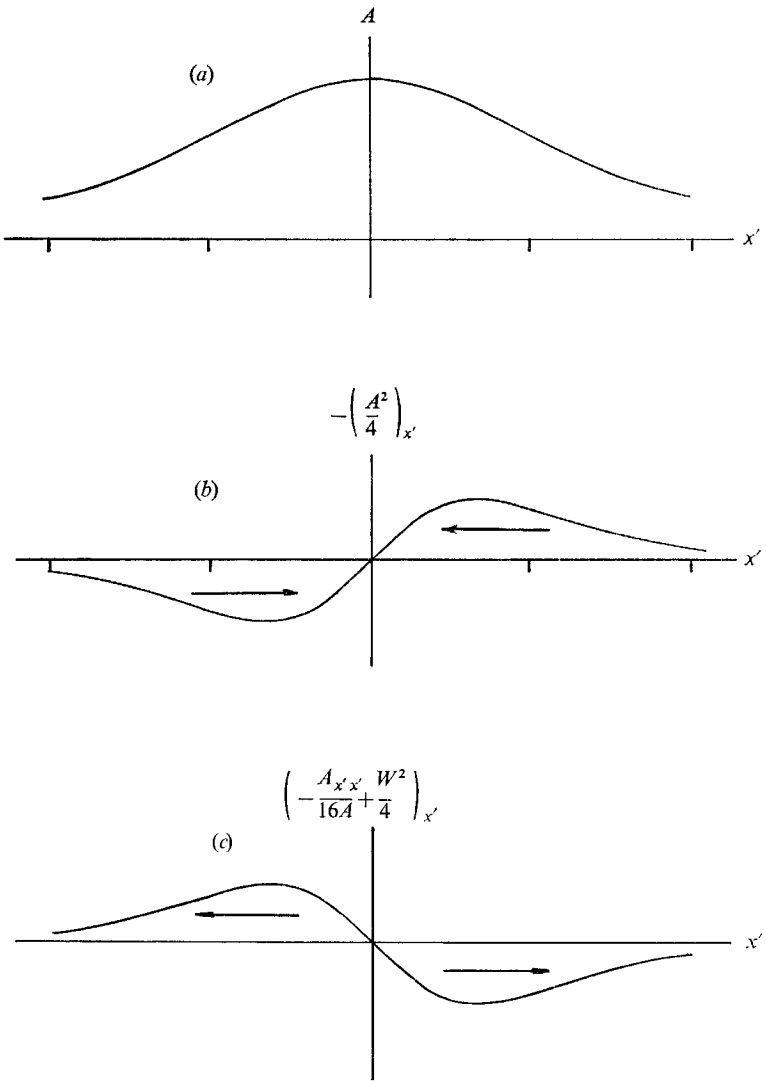

FIGURE 3. Sketch illustrating effects of amplitude dispersion and frequency dispersion at small time: (*a*) initial profile A *vs* x', $W = 0$; (*b*) amplitude dispersion $-(\partial/\partial x')\,\frac{1}{4}A^2$ *vs.* x'; (*c*) frequency dispersion

$$\frac{\partial}{\partial x'}\left(\tfrac{1}{4}W^2 - \frac{1}{16}\frac{A_{x'x'}}{A}\right) \textit{vs.}\ x';$$

arrows show direction of energy flux.

precise behaviour in this region should in principle be treated by using a better approximation involving still higher derivatives. However, since this is a region of essentially no motion, in contrast with the breaking crest of a shallow water wave, a refined treatment of this local singularity is unlikely to alter the overall picture drastically. Although further development of the side groups has not been computed here, it is reasonable to expect that they undergo a similar process of disintegration and stabilization. We stress that since these permanent envelopes propagate at the original group velocity whatever the amplitude, the larger groups have no means of escaping or overtaking the smaller ones; this feature is quite different from shallow water waves under similar initial conditions (see Gardner *et al.* 1967, Madsen & Mei 1969).

6. Periodic modulation of Stokes waves

As some of the conclusions by Benjamin & Feir (1967) on the initial instability are needed here, we find it convenient to present a very short derivation. For small disturbances the linearized equations (2.6) apply. If a side-band disturbance of the kind $(\alpha, \beta) = (\hat{\alpha}, \hat{\beta}) \exp\{i(\kappa x' - \Omega t')\}$ is assumed, the eigenvalue condition gives $\Omega = \frac{1}{8}\kappa(\kappa^2 - 8)^{\frac{1}{2}}$; thus $\kappa < 2^{\frac{3}{2}}$ for instability. From this the growth rate is found to be $\alpha_{t'}/\alpha = \beta_{t'}/\beta = \frac{1}{8}\kappa(8 - \kappa^2)^{\frac{1}{2}}$. The maximum growth rate occurs when $\kappa = 2$ for which

$$\alpha_{t'}/\alpha = \beta_{t'}/\beta = \tfrac{1}{2} \quad \text{and} \quad \hat{\alpha}/\hat{\beta} = i. \tag{6.1}$$

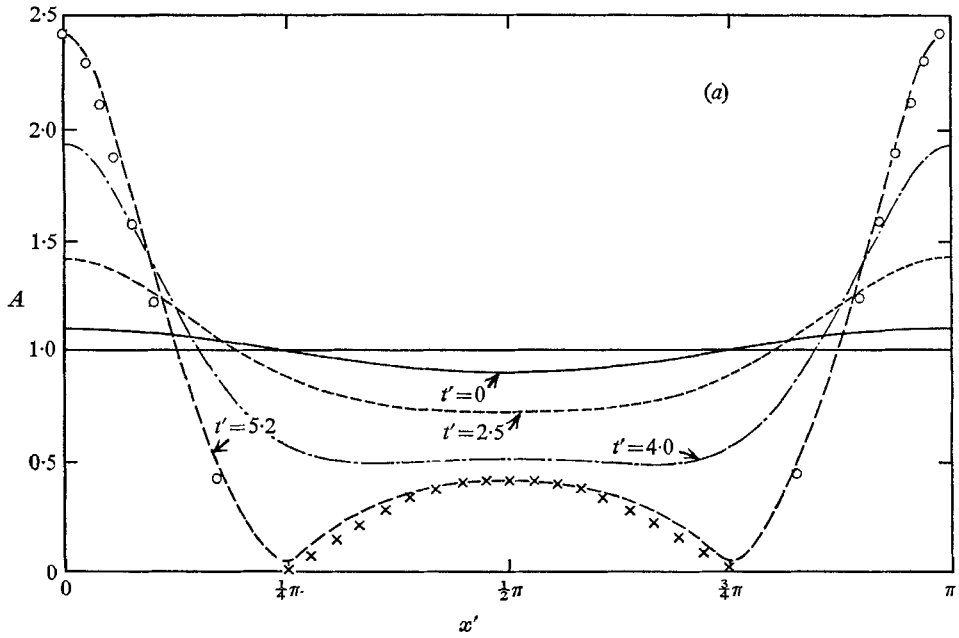

FIGURE 4. Evolution of an unstable Stokes wave (initial conditions: $A = 1 + (0{\cdot}1)\cos 2x'$, $W = (0{\cdot}1)\sin 2x'$ at $t = 0$.) $\Delta x' = \pi/100$, $\Delta t' = 0{\cdot}001$, $N = 100$. × × ×, ○○○, permanent periodic envelopes; (*a*) amplitude A; (*b*) wave-number spread W; (*c*) growth rate of crest or trough (——), of net amplitude between crest and trough (——).

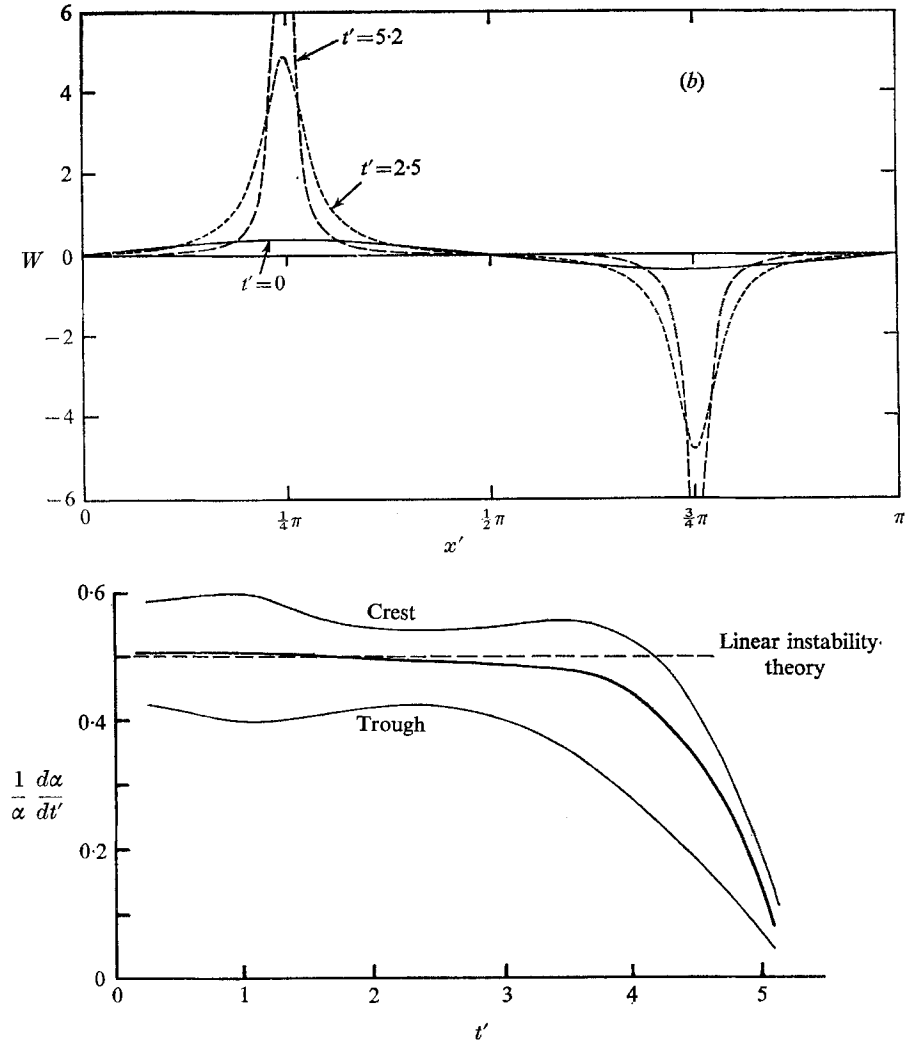

FIGURE 4(*b*), (*c*). For legend see previous page.

We now consider the non-linear problem and select the initial modulation to correspond to the maximum growth rate. Noting that $\hat{\alpha}$ and $\hat{\beta}$ are out of phase by $\frac{1}{2}\pi$ we select

$$A = 1 + 0{\cdot}1 \cos 2x', \quad W = 0{\cdot}1 \sin 2x'. \tag{6.2}$$

The numerical results are given in figures 4(*a*), (*b*) and (*c*). Initially as the envelope amplifies, the crest and the trough (the latter is defined here as the midpoint between two successive initial crests) grow at different rates (figure 4(*c*)). The growth rate of the wave height between the crest and trough is, of course, $\frac{1}{2}$. After a certain time nodes are formed with separated groups settling down to permanent forms of different dimensions. Wave-number peaks and phase jumps appear near the nodes. These groups again propagate at the same speed, as each is a cnoidal wave of type (*b*) in figure 1.

7. Discussion of Feir's pulse experiment

Measured results were published by Feir for the situation studied in §5. In particular, time records of six pulses, taken at 4 ft. and 28 ft. from the wave-maker, are available for increasingly sharp initial envelopes (Feir 1967, figure 3). Although all the envelopes generated at the wave-maker are symmetrical and the frequency constant, the steeper ones have already become forward-leaning at 4 ft., due perhaps to the fact that the amplitude dispersion has longer time to manifest itself in the front of the pulse than in the lee. Separation into groups is evident in five of the six records. Two aspects in these experiments need to be pointed out before attempting quantitative comparison with the theory.

First, although the physical distance between two measuring stations is the same for all runs (24 ft.), due to the difference of initial amplitudes, the down-stream records actually correspond to different stages of development. This is made clear by considering the dimensionless time between the passage of pulse peak at the 4 ft. and the 28 ft. stations, i.e.

$$t'_{28'} = (\bar{k}\bar{a})_4^2 (2\bar{\omega}^2/g)\,(28-4), \tag{7.1}$$

where the maximum amplitude at the 4 ft. station is taken as $\bar{a}$. Since $\bar{\omega}$ and $\bar{k}$ are the same in all runs, larger initial $\bar{a}$ corresponds to larger values of t'_{28}, and hence later stages of evolution; these values are listed in table 1 in the same sequence as appeared in the original paper.

Second, viscous effects in all cases are significant, resulting in the loss of nearly one-half of the total energy, which Feir (private communication) ascribed to be partly due to the side-wall boundary layers and partly due to free-surface contamination. Now the degree of contamination is hard to assess for theoretical purposes, we shall only deal with the problem of viscous damping empirically as follows.

We define a damping coefficient, assumed constant, by comparing the energy loss between two given stations; this is done by modifying the energy equation (2.3a) (omitting the order symbol ϵ):

$$\left(\frac{\partial}{\partial t} + \bar{C}_g \frac{\partial}{\partial x}\right) a^2 + \frac{d\bar{C}_g}{dk} \frac{\partial}{\partial x} a^2 = -\sigma^* a^2. \tag{7.2}$$

At a fixed x, we integrate the preceding equation with respect to t over $(-\infty, \infty)$ using the fact that $a(x, \pm\infty) = 0$ for pulse experiments we have

$$\bar{C}_g \frac{d}{dx} E_T = -\sigma^* E_T, \quad E_T = \int_{-\infty}^{\infty} a^2 dt.$$

Integrating from x_0 to x_1 we have

$$\sigma^* = -\bar{C}_g \frac{\log\left[E_T(x_1)/E_T(x_0)\right]}{x_1 - x_0}. \tag{7.3}$$

In dimensionless form (7.2) becomes

$$\frac{\partial A^2}{\partial t'} + \frac{\partial}{\partial x'}(-\tfrac{1}{2} W A^2) = -\sigma A^2, \tag{7.4}$$

where

$$\sigma = \sigma^*/\bar{\omega}(\bar{k}\bar{a})^2. \tag{7.5}$$

The values of σ for all runs are computed from the published records by taking $x_0 = 4$ ft., $x_1 = 28$ ft. measured from the wave-maker, and are also listed in table 1. Thus the percentage energy damped per unit time (scale $\sim (\omega(\bar{k}\bar{a})^2)^{-1}$) is more severe in cases of smaller initial amplitude.

Run	$(\bar{k}\bar{a})_{4'}$	$(\bar{k}\bar{a})_{28'}$	$t'_{28'}$	σ
1	0·064	0·034	1·5	0·562
2	0·098	0·068	3·5	0·193
3	0·114	0·084	4·8	0·158
4	0·151	0·108	8·4	0·088
5	0·207	0·132	15·8	0·061
6	0·227	0·173	19·0	0·043

TABLE 1. Important parameters in Feir's experiment

We have replotted Feir's records $\eta(t)$ in dimensionless variables $A(x')$ using the relation between x' and t for fixed x (cf. (2.4)). For comparison a solitary envelope of equal $A_{\max}$, i.e. $A/A_{\max} = \operatorname{sech} 2^{\frac{1}{2}} A_{\max} x'$, is superimposed on the main pulse at both stations. For runs 1, 2 and 3 where the envelopes are roughly symmetrical, the damping is strong and the duration of evolution is short, the dominant feature is an attenuation in amplitude. The pulse profile of run 1 is somewhat sharper than the comparison pulse of permanent form at 4 ft. and of course remains so at 28 ft., after relatively the shortest travel time. The profiles of

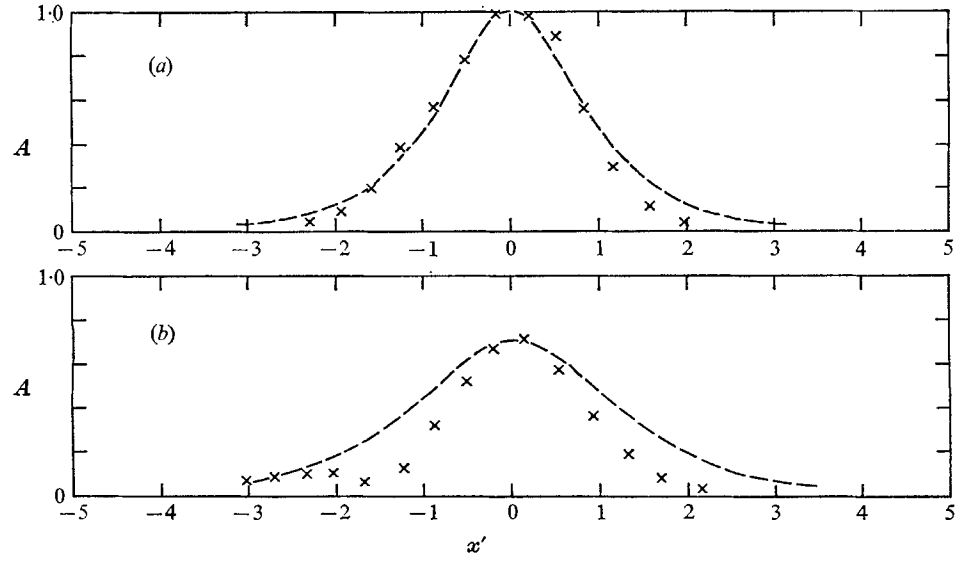

FIGURE 5. Dimensionless plot of run 3 (Feir 1967). × × ×, measured envelope; - - -, permanent pulse of equal height. (*a*) $t' = 0$, corresponding to probe at 4 feet from wave-maker; (*b*) $t' = 4.8$, corresponding to probe at 28 ft. from wave-maker.

runs 2 and 3 are essentially of permanent form at 4 ft.; but they also become sharper than the comparison profiles at 28 ft., as illustrated by figures 5 (*a*) and (*b*) for run 3. This is simply a manifestation of the dominating influence of damping at small time, in particular, $(1/A)\partial A/\partial t' \cong -\sigma$ from (7.4). Now since σ should be approximately uniform in x for small time, a permanent pulse of maximum amplitude A_0 at the upstream station will decay to

$$A_2 \cong cA_0 \operatorname{sech}(2^{\frac{1}{2}}A_0 x')$$

downstream, where $c = 1 - \Delta A/A_0 \cong$ constant < 1. However, the comparison permanent pulse is given by

$$A_2' = cA_0 \operatorname{sech}(2^{\frac{1}{2}}cA_0 x').$$

Clearly, since $c < 1$, we must have $A_2/A_2' \leqslant 1$ for all x' with equality for $x' = 0$ only.

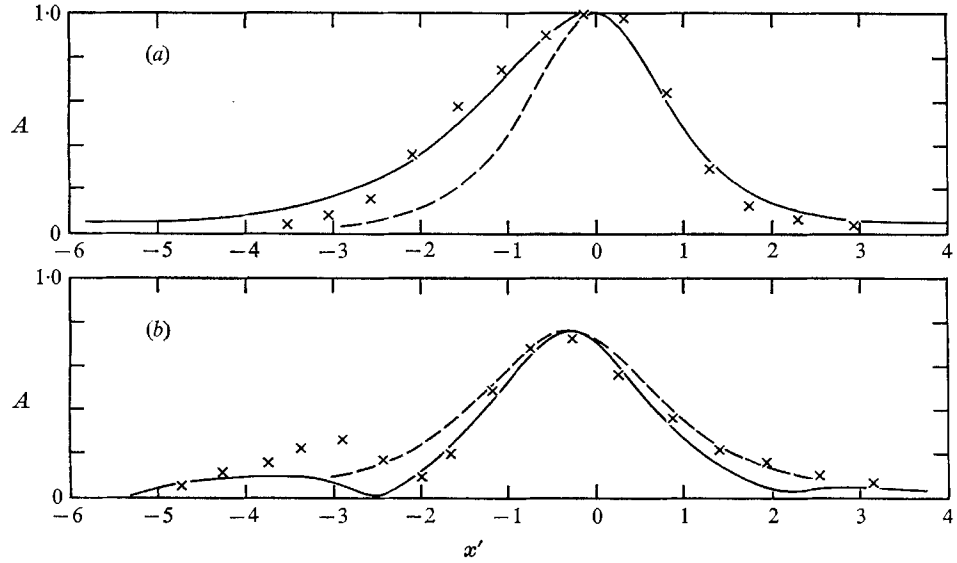

FIGURE 6. Comparison between measured and computed envelope for run 4 (Feir 1967). × × ×, measured envelope; - - -, permanent pulse of equal height; ——, computed envelope with damping. $\Delta x' = 0{\cdot}1$, $\Delta t' = 0{\cdot}01$.

Runs 4, 5 and 6 are decidedly asymmetrical with the front close to, but the back flatter than, a solitary envelope (see figure 6 for run 4). Due to relatively low damping and long time of evolution in each run the main pulse at 28 ft. is approximately a solitary envelope, in qualitative agreement with calculations based on zero damping (§ 5). Furthermore, the presence of separated pulses is certain only in the lee, and not on both sides of the main pulse. This is likely the combined consequence of (i) some wave-number variation at the initial station at 4 ft., and (ii) side-wall boundary layers and surface contamination. The first cause can in principle be checked by solving (2.3*a*, *b*) for a genuine initial-boundary-value problem accounting for the motion of the wave-maker; this, however, demands significant modification of numerical work. A simpler alternative would be to

infer the wave-number variation from analysis of experimental data, which is not available at present. According to a linearized theory for two-dimensional waves (Hunt 1964), the bottom boundary layer affects the real and the imaginary parts of the dispersion relation at the order $O(k\delta)$, i.e.

$$\left.\begin{aligned}\omega_r/\omega_0 &= 1-\tfrac{1}{2}k\delta/2\sinh 2kh+O(k\delta)^3,\\ \omega_i/\omega_0 &= -k\delta/2\sinh 2kh+O(k\delta)^2,\end{aligned}\right\} \tag{7.6a,b}$$

where $\omega_0 = (gk\tanh kh)^{\frac{1}{2}}$, $\delta = (2\nu/\omega_0)^{\frac{1}{2}}$, and k real. The side walls, being rigid as the bottom, are likely to exert a similar influence with the coefficients in (7.6a, b), $(-2\sinh 2kh)^{-1}$, replaced by some functions depending on kb (b = tank width). This is indeed so for ω_i/ω_0 ($\sim$ damping rate) (Hunt 1952):

$$\omega_i/\omega_0 = -\frac{k\delta}{2}\left(\frac{1}{kb}+\frac{1}{\sinh 2kh}\right).$$

Note, however, that the effect of the side walls is comparatively stronger ($O(kb)^{-1}$) than that of the bottom ($O(e^{-2kh})$) for large kb or kh. Now if ω_r/ω_0 is similarly influenced, a term of $O(k\delta/kb)$ would not be totally negligible from (1.4) over a long distance or time, as the Stokes term $\frac{1}{2}(ka)^2$ is also small.† No theory on this or the surface contamination is yet known.

In view of the above difficulties, we do not attempt a complete comparison between theory and experiment here. Instead an initial profile is chosen to fit the measured envelope and the initial wave-number is taken to be constant, i.e. $W(x, 0) = 0$. Calculations are then made on the bases of (7.4) and (2.5b), i.e. viscous effect on energy, but not on phase, is considered. Figure 6 shows a typical result made for run 4. It is seen that the predicted values and experiment are in fairly good accord over the main group, though not over the side groups. The secondary group in the lee is larger than the one in front of the main group, in qualitative agreement with the observations.

Decisive checks may be made by further reduction of viscous effects in larger tanks. Nevertheless, the evidence discussed so far is strongly in favour of the present theory in which the envelope remains dispersive as its constituent waves.

We wish to express our sincere thanks to Dr C. J. R. Garrett for several perceptive comments and suggestions on an earlier draft of this paper. The financial support by the Coastal Engineering Research Centre, U.S. Army Corps of Engineers (Contract DACW 72-68-C-0012) is also gratefully acknowledged.

REFERENCES

Benjamin, T. B. & Feir, J. E. 1967 *J. Fluid Mech.* **27**, 417.

Benney, D. J. & Newell, A. C. 1967 *J. Math. Phys.* **46**, 133.

Chu, V. H. & Mei, C. C. 1970*a* *Tech. Rep.* 125, *Water Res. Hydro. Lab., Mass. Inst. Tech.*

Chu, V. H. & Mei, C. C. 1970*b* *J. Fluid Mech.* **41**, 873.

Feir, J. E. 1967 *Proc. Roy. Soc.* A **299**, 54.

† In Feir's experiments the typical values are: $\omega_0 = 5\pi$, $ka = 0{\cdot}1$, $kb = 15$, $k\delta = 0{\cdot}01$. Hence $k\delta(kb)^{-1}(ka)^{-2} = O(10^{-1})$. Note from table 1 that the damping rate is of comparable magnitude: $0{\cdot}04 < \sigma < 0{\cdot}6$.

GARDNER, C. S. GREENE, J. M., KRUSKAL, M. O. & MIURA, R. M. 1967 *Phys. Review Letters*, **19**, 1095.

HOWE, M. S. 1967 *J. Fluid Mech.* **30**, 497.

HOWE, M. S. 1968 *J. Fluid Mech.* **32**, 779.

HUNT, J. N. 1952 *La Houille Blanche*, **7**, 836.

HUNT, J. N. 1964 *La Houille Blanche*, **6**, 685.

LIGHTHILL, M. J. 1965 *J. Inst. Maths. Applics.* **1**, 296.

LIGHTHILL, M. J. 1967 *Proc. Roy. Soc.* A **311**, 371.

MADSEN, O. S. & MEI, C. C. 1969 *J. Fluid Mech.* **39**, 781.

MORSE, P. M. 1948 *Vibration and Sound*. McGraw-Hill.

RICHTMYER, R. D. 1964 *Difference Methods for Initial Value Problems*. Interscience.

WHITHAM, G. B. 1967 *J. Fluid Mech.* **27**, 399.